Monitoring statistics of the ERS-2 scatterometer for ESA

cycle 86

(Project Ref. 15988/02/I-LG)

Hans Hersbach
European Centre for Medium-Range Weather Forecasts,
Shinfield Park, Reading, RG2 9AX, England
Tel: (+44 118) 9499476, e-mail: dal@ecmwf.int

September 3, 2003

1 Introduction

From 12 December 2001 onwards, ESRIN redistributes ERS-2 scatterometer data to a selected group of users. On 4 February 2003, a new processor, ESACA, was introduced. It is an upgrade of the existing LRDPF and includes new scatterometer processing algorithms that anticipate errors in the satellites yaw attitude control. It was installed for Kiruna station only and is currently running in test phase. On 22 June 2003, both LBR tape recorders failed, with the consequence that from that date onwards only data has been received for regions for which the satellite has direct visual contact with a ground station. For Kiruna station this means restriction to the North Atlantic.

The quality of this experimental product was monitored at ECMWF for cycle 86. Results were compared to those obtained from previous cycles including all received data (i.e., global coverage). In addition, a comparison was also made with data in cycle 85 restricted to the coverage as observed during cycle 86. It was found that this is accurately represented by the criterion:

$$(\mathrm{lat} + 0.5\,\mathrm{lon} \geq 43) \qquad \text{and} \qquad (\mathrm{lat} - 0.3\,\mathrm{lon} \geq 49),$$

where latitude (lat) and longitude (lon) are both in degrees (the area north of the solid lines in Figure 9, from now on denoted by the 'regional set').

The scatterometer data was not used in the 4D-Var data assimilation system at ECMWF.

During cycle 86, data was received between 09:45 UTC 16 July and 19:31 UTC 11 August 2003. Before this period, i.e., from 8 July to 16 July 2003, no data was available, which was connected to the failure of the LBR tape recorders. Besides, due to the reception of data from Kiruna station only, usually no data was received for the 6-hourly data periods centered around 00 UTC. In case data was received for 00 UTC, data volumes were low. Occasionally low volumes for 18 UTC and 6 UTC can also be attributed to the lack of data from the other stations.

Time series for the asymmetry between the incidence angles of the fore and aft beam (related to yaw attitude errors), show several peaks, with amplitudes up to 3.5 degrees. No clear signals for enhanced solar activity were observed.

Due to very low data volumes received during cycle 86, it has been difficult to quantify the potential quality of the wind product. It seems to be stable, since only small patches of suspected poor quality data were observed. The standard deviation compared to ECMWF first-guess winds (FGAT) have decreased as compared to the regional set of cycle 85, however, bias levels have become more negative. The number of collocations of low UWI winds with high FGAT winds has increased; a sign of quality degradation. The quality of the UWI wind direction was better to that for the regional data received during cycle 85. In summary the results on the evolution of data quality are mixed.

The ECMWF assimilation system was not changed during cycle 86.

2 ERS-2 statistics from 8 July to 11 August 2003

2.1 Sigma0 bias levels

The average sigma0 bias levels (compared to simulated sigma0's based on ECMWF model first-guess winds) stratified with respect to antenna beam, ascending or descending track and as function of incidence angle (i.e. across-node number) is displayed in Figure 1. Compared to global data sets received for earlier cycles, data volumes are much lower, resulting in much larger error bars (displayed in Figure 1 as well).

Compared to the global set in cycle 85, bias levels have become more negative (up to 0.3 dB). Internode differences seem to have grown as well, although they are within the (large) error bars. Compared to the regional set in cycle 85 (results not shown), bias levels have become more negative as well. Therefore, the trend is realistic, and is not connected to a change in data coverage.

The data volume of ascending tracks is smaller than that of descending tracks, which must be a consequence of the geographical situation of the visibility range of Kiruna station.

2.2 Incidence angles

For ESACA, across-node binning is, like the old processor, retained on a 25km mesh. From simple geometrical arguments it follows that variations in yaw attitude will lead to asymmetries between the incidence angles of the fore and aft beam. Indeed, this has been observed. Figure 2 gives a time evolution of this asymmetry, showing rapid variations, which are typical for yaw attitude errors. Peaks are lower than those observed during previous cycles.

2.3 Distance to cone history

The distance to the cone history is shown in Figure 3. Most of the peaks are due to low data volumes that now occur on a daily basis. For the remaining 6-hourly cycles data volumes are much lower than before as well. This makes it very difficult to identify peaks in the cone history with instrument anomalies, since statistical fluctuations are too large. The same picture emerges for the regional data set in cycle 85 (not shown), while its global data set does allow for an identification of instrument anomalies. In future it may be necessary to average data over longer periods, e.g., over 24 hours.

Compared to cycle 85, the average cone distance has increased. Although part of it is induced by the change in data coverage (revealed by a similar analysis for the regional set of cycle 85), the remaining increase must be related to a change in the characteristics of the data. Especially for lower nodes average levels have become higher. Only for the highest nodes average cone distances were smaller than those for the regional set of cycle 85, though higher than for the global set of cycle 85. Averaged over all nodes (see top panel of Figure 8), the level has increased from 1.05 (cycle 85, global set), via 1.18 (cycle 85, regional set) to 1.35 (cycle 86).

2.4 UWI minus First-Guess wind history

In Figure 4, the UWI minus ECMWF first-guess wind-speed history is plotted.

Like it is the case for the history of the cone distance, the low data volumes make it difficult to separate instrument anomalies from numerical noise. Averages over periods longer than 6 hours may be necessary in future.

Average bias levels and standard deviations of UWI winds relative to FGAT winds are displayed in Table 1. From this it is seen that, compared to the regional set of cycle 85, the average bias level has become considerably more negative (-0.96 m/s, was -0.72 m/s for regional, respectively -0.80 m/s for global coverage in cycle 85). The large wind bias at the lower nodes has compared to the regional set of cycle 85 become more negative as well (-1.54, was -1.45 m/s). The standard deviation, however, has improved (average 1.45 m/s, was 1.51 m/s). It is also lower than for the global data set in cycle 85 (1.59 m/s) since this set contains extremer wind conditions in the southern hemisphere.

Like for ESACA data received for cycle 85, the at ECMWF inverted CMOD4 winds do not match the UWI winds. The quality of these CMOD4 winds is considerably higher than that of the UWI winds (standard deviation of 1.37 m/s versus 1.45 m/s). In contrast to previous cycles CMOD4 winds are also of higher quality than winds determined on the basis of CMOD5 (shown below). The same applies for the regional set of cycle 84.

For cycle 86 the (scatterometer - model) direction standard deviations were ranging between 20 and 40 degrees (Figure 5). Sharp peaks are the result of low data volumes. For de-aliased CMOD4 winds values between 20 and 30 degrees are most common. On average (see Table 1), the quality of the UWI wind direction is higher

	cycle 85, global		cycle 85, regional		cycle 86	
	UWI	CMOD4	UWI	CMOD4	UWI	CMOD4
speed STDV	1.59	1.44	1.51	1.40	1.45	1.37
node 1-2	1.50	1.46	1.39	1.39	1.42	1.43
node 3-4	1.40	1.38	1.34	1.31	1.37	1.36
node 5-7	1.49	1.37	1.41	1.31	1.38	1.31
node 8-10	1.60	1.39	1.50	1.33	1.39	1.27
node 11-14	1.61	1.40	1.52	1.34	1.44	1.31
node 15-19	1.58	1.41	1.57	1.42	1.50	1.38
speed BIAS	-0.80	-0.85	-0.72	-0.70	-0.96	-0.97
node 1-2	-1.63	-1.69	-1.45	-1.48	-1.54	-1.58
node 3-4	-1.19	-1.20	-1.09	-1.08	-1.25	-1.25
node 5-7	-0.82	-0.82	-0.78	-0.73	-0.98	-0.96
node 8-10	-0.57	-0.60	-0.48	-0.45	-0.74	-0.75
node 11-14	-0.54	-0.60	-0.44	-0.42	-0.70	-0.73
node 15-19	-0.62	-0.69	-0.44	-0.42	-0.79	-0.82
direction STDV	25.9	18.6	31.9	18.2	25.3	18.5
direction BIAS	1.2	0.7	-2.1	-3.2	-3.7	-4.3

Table 1: Biases and standard deviation of ERS-2 versus ECMWF FGAT winds in m/s for speed and degrees for direction

than that for data received during the regional set of cycle 85 (25.3 degrees, was 31.9 degrees, see also lower panel of Figure 8), and also slightly better than for the global set of cycle 85 (25.9 degrees). The quality of the de-aliased CMOD4 wind direction is stable (18.5 degrees versus 18.2 respectively 18.6 degrees).

In Figure 9 all locations are plotted for which UWI winds were more than 6 m/s weaker than the FGAT winds (rather than 8 m/s, as plotted for previous cycles). There are no clear signs for instrument anomalies (such as occurred for cycle 83, and for cycles before the introduction of the ESACA processor), in which case large parts of tracks would appear in Figure 9.

For two cases from Figure 9, wind fields are shown in Figure 10. In the top panel (south of Greenland) both scatterometer winds and FGAT winds look sensible. However, for the lower panel (north-west from Norway) there is a small unrealistic patch of UWI winds.

2.5 Scatter plots

Scatterplots of model 10 m first-guess winds versus ERS-2 winds are displayed in Figures 11 to 14. Values of standard deviations and biases are slightly different from those displayed in Table 1. Reason for this is that, for plotting purposes, the in 0.5 m/s resolution ERS-2 winds have been slightly perturbed (increases scatter with 0.02 m/s), and that zero wind-speed ERS-2 winds have been excluded (decreases scatter with about 0.05 m/s). These scatterplots elucidate trends described in the previous subsection.

Like for cycle 85, the quality of the CMOD4 winds (Figure 13) is higher than that of the UWI winds (Figure 11). This seems to be especially true for strong winds. Values of standard deviations for both UWI and CMOD4 winds are much lower to those for the global set of cycle 85. However, this difference is deceptive, since cycle 86 did not include any strong winds on the southern hemisphere. Nevertheless, compared to the regional data set of cycle 85, the standard deviation relative to FGAT winds has decreased (for UWI winds: 1.47 m/s, was 1.52 m/s) Bias levels, however, have become more negative (-0.96 m/s, was -0.72 m/s).

The average bias of the UWI wind direction has become more negative (Figure 12), which appears to be mainly induced by the change in coverage (-3.9 degrees, was -2.74 and 0.50 degrees for the regional respectively global set). Limited to the regional set, the standard deviation of wind direction has decreased somewhat (23.4 degrees, was 28.1 for the regional, and 23.6 for the global set).

There were more collocations of low UWI winds and high ECMWF FGAT winds (Figure 11) than there were for both the global and regional set of cycle 85. These usually originate from errors in yaw attitude control.

Winds derived on the basis of CMOD5 are displayed in Figure 13. Compared to the regional set of cycle 85, the bias level has become more negative (-0.72 m/s, was -0.44 m/s) although the standard deviation improved somewhat (1.43 m/s, was 1.45 m/s). For the first time of its monitoring, CMOD5 winds are of lower quality than the CMOD4 (Figure 13). This is also observed for the regional set of cycle 85. The reason for this is to be investigated.

Figure Captions

Figure 1: Ratio of $< \sigma_0^{0.625} > / <$ CMOD4(FirstGuess)$^{0.625} >$ converted in dB for the fore beam (solid line), mid beam (dashed line) and aft beam (dotted line), as a function of incidence angle for descending and ascending tracks. The thin lines indicate the error bars on the estimated mean. First-guess winds are based on the in time closest (+3h, +6h, +9h, or +12h) T511 forecast field, and are bilinearly interpolated in space.

Figure 2: Time series of the difference in incidence angle between the fore and aft beam.

Figure 3: Mean normalized distance to the cone computed every 6 hours for nodes 1-2, 3-4, 5-7, 8-10, 11-14 and 15-19 (solid curve close to 1 when no instrumental problems are present). The dotted curve shows the number of incoming triplets in logarithmic scale (1 corresponds to 60,000 triplets) and the dashed one indicates the fraction of complete sea-located triplets rejected by ESA flags, or by the wind

inversion algorithm (0: all data kept, 1: no data kept).

Figure 4: Mean (solid line) and standard deviation (dashed line) of the wind speed difference UWI - first guess for the data retained by the quality control.

Figure 5: Same as Fig. 4, but for the wind direction difference. Statistics are computed only for wind speeds higher than 4 m/s.

Figures 6 and 7: Same as Fig. 5 and 6 respectively, but for the de-aliased CMOD4 data.

Figure 8: Evolution of the performance of the ERS-2 scatterometer averaged over 5-weekly cycles from 12 December 2001 (cycle 69) to 11 August 2003 (end cycle 86) for the UWI product (solid, star) and de-aliased winds based on CMOD4 (dashed, diamond). For cycle 85 two values are plotted; the first value for the global set, the second one for the regional set. Dotted lines represent values for cycle 59 (5 December 2000 to 17 January 2001), i.e. the last stable cycle of the nominal period. From top to bottom panel are shown the normalized distance to the cone (CMOD4 only) the standard deviation of the wind speed compared to FGAT winds, the corresponding bias (for UWI winds the extreme inter-node averages are shown as well), and the standard deviation of wind direction compared to FGAT.

Figure 9: Locations of data during cycle 86 for which UWI winds (top panel), respectively CMOD5 winds (lower panel) are more than 6 m/s weaker than the collocated FGAT winds. The area north of the two solid lines indicates the area for which data was received during cycle 86. It corresponds to the direct visibility range of Kiruna station.

Figure 10: UWI or CMOD5 wind vectors (red) and collocated FGAT wind vectors (blue) near Greenland for 8 August 2003 (top panel) and near Norway for 30 July 2003 (lower panels).

Figure 11: Two-dimensional histogram of first guess and UWI wind speeds, for the data kept by the quality control, however, disregarding the level of k_p. Circles denote the mean values in the y-direction, and squares those in the x-direction.

Figure 12: Same as Fig. 11, but for wind direction. Only wind speeds higher than 4m/s are taken into account.

Figure 13: Same as Fig. 11, but for de-aliased CMOD4 winds.

Figure 14: Same as Fig. 11, but for de-aliased CMOD5 winds.

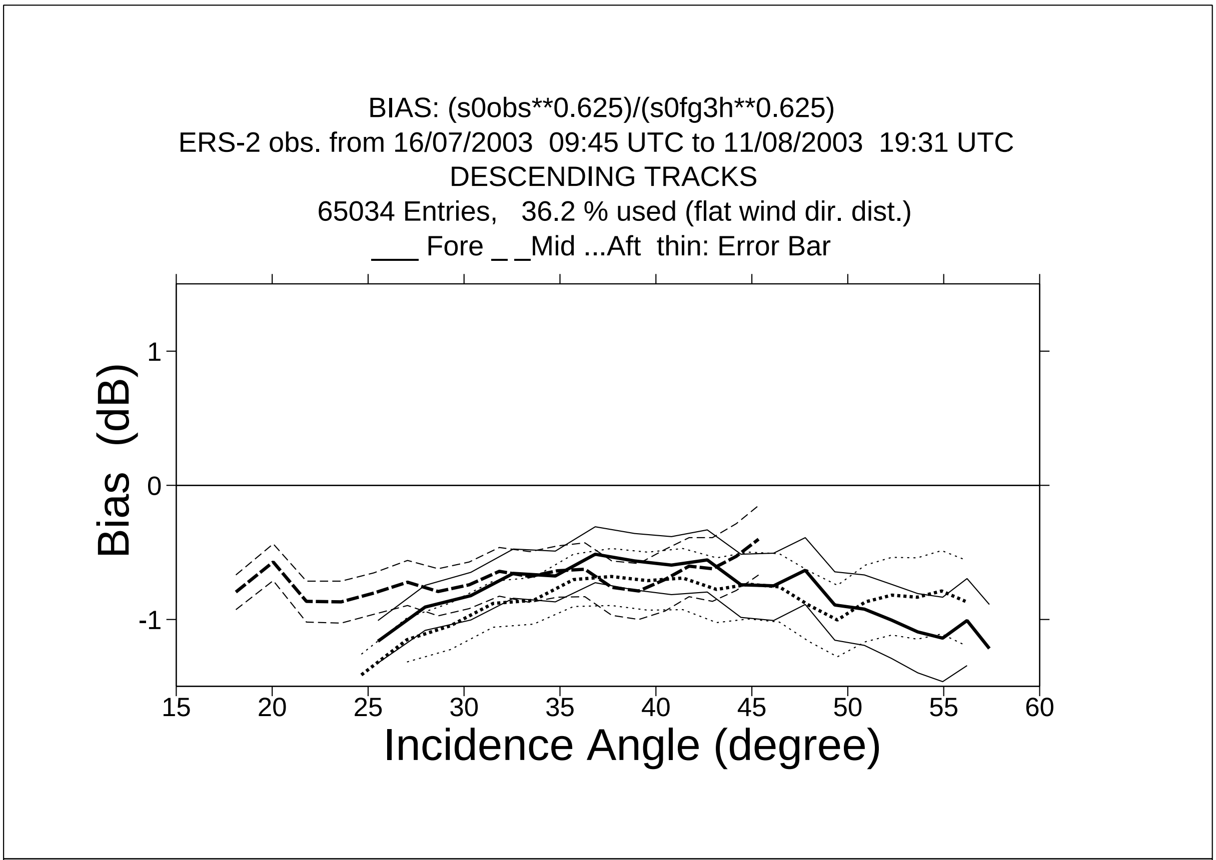
BIAS: (s0obs**0.625)/(s0fg3h**0.625)
ERS-2 obs. from 16/07/2003 09:45 UTC to 11/08/2003 19:31 UTC
DESCENDING TRACKS
65034 Entries, 36.2 % used (flat wind dir. dist.)
___ Fore _ _Mid ...Aft thin: Error Bar
Bias (dB)
1
0
-1
15
20
25
30
35
40
45
50
55
60
Incidence Angle (degree)

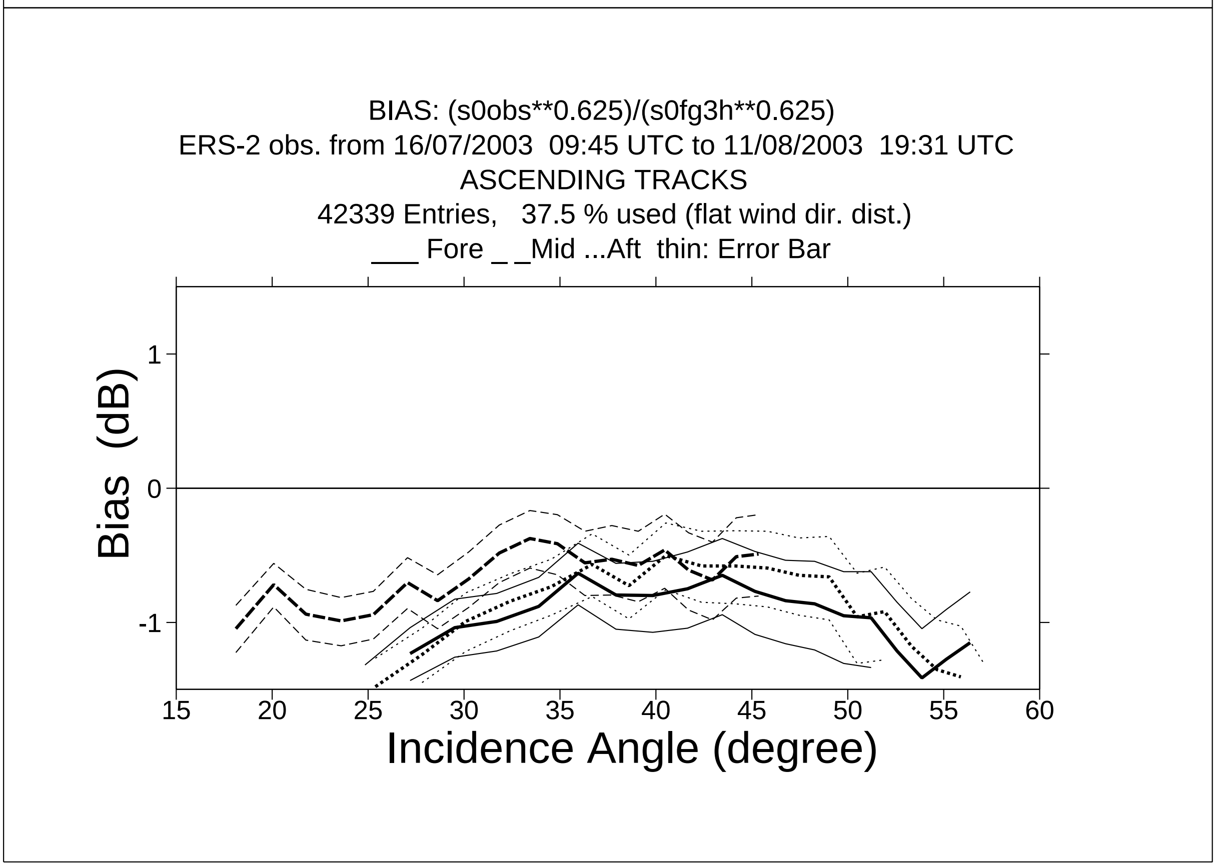
BIAS: (s0obs**0.625)/(s0fg3h**0.625)
ERS-2 obs. from 16/07/2003 09:45 UTC to 11/08/2003 19:31 UTC
ASCENDING TRACKS
42339 Entries, 37.5 % used (flat wind dir. dist.)
___ Fore _ _Mid ...Aft thin: Error Bar
Bias (dB)
1
0
-1
15
20
25
30
35
40
45
50
55
60
Incidence Angle (degree)

Figure 1

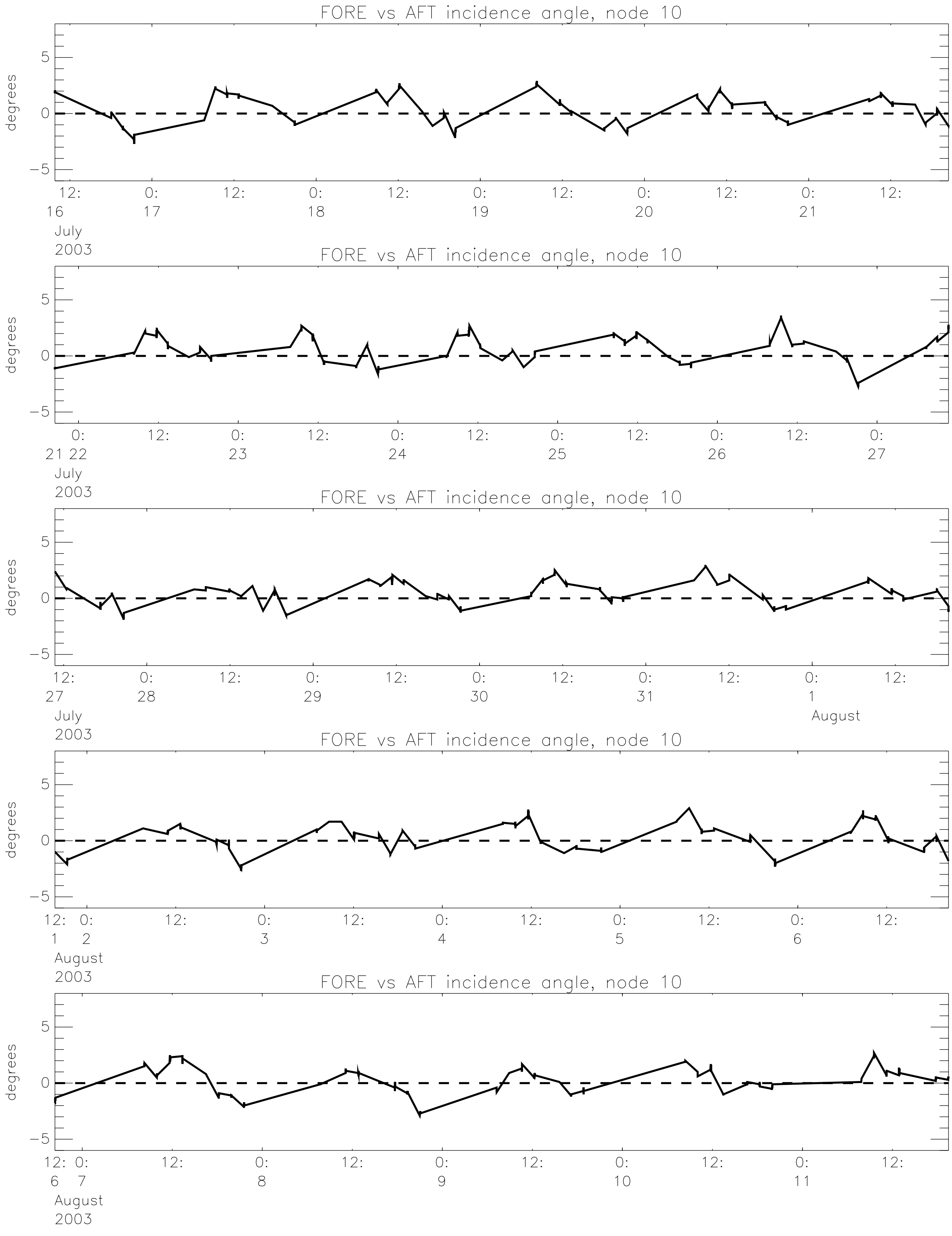
FORE vs AFT incidence angle, node 10
degrees
5
0
−5
12: 0: 12: 0: 12: 0: 12: 0: 12: 0: 12:
16 17 18 19 20 21
July
2003
FORE vs AFT incidence angle, node 10
degrees
5
0
−5
0: 12: 0: 12: 0: 12: 0: 12: 0: 12: 0:
21 22 23 24 25 26 27
July
2003
FORE vs AFT incidence angle, node 10
degrees
5
0
−5
12: 0: 12: 0: 12: 0: 12: 0: 12: 0: 12:
27 28 29 30 31 1
July
August
2003
FORE vs AFT incidence angle, node 10
degrees
5
0
−5
12: 0: 12: 0: 12: 0: 12: 0: 12: 0: 12:
1 2 3 4 5 6
August
2003
FORE vs AFT incidence angle, node 10
degrees
5
0
−5
12: 0: 12: 0: 12: 0: 12: 0: 12: 0: 12:
6 7 8 9 10 11
August
2003

Figure 2

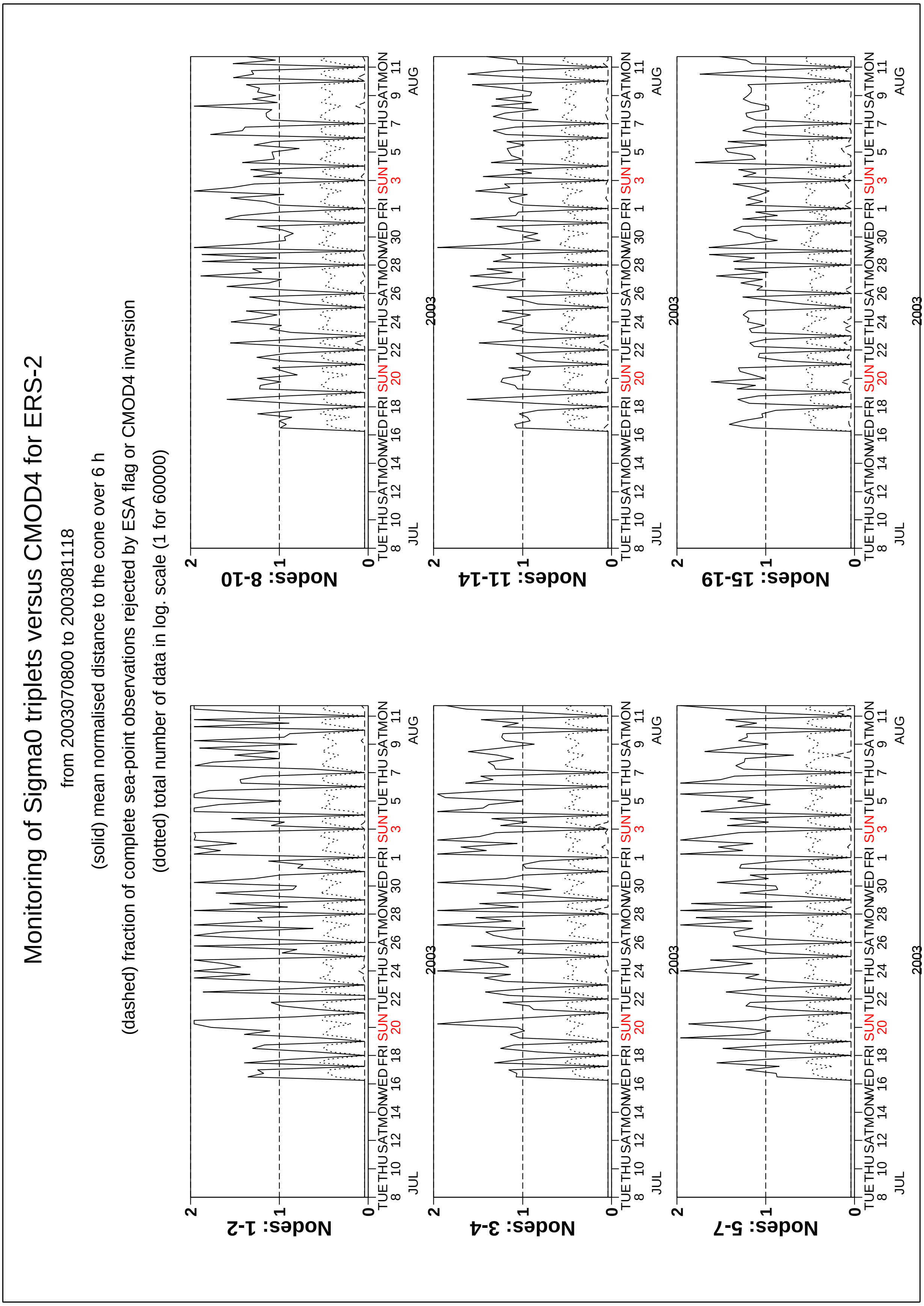
Monitoring of Sigma0 triplets versus CMOD4 for ERS-2
from 2003070800 to 2003081118
(solid) mean normalised distance to the cone over 6 h
(dashed) fraction of complete sea-point observations rejected by ESA flag or CMOD4 inversion
(dotted) total number of data in log. scale (1 for 60000)
Nodes: 1-2
Nodes: 3-4
Nodes: 5-7
Nodes: 8-10
Nodes: 11-14
Nodes: 15-19
JUL
AUG
2003

Figure 3

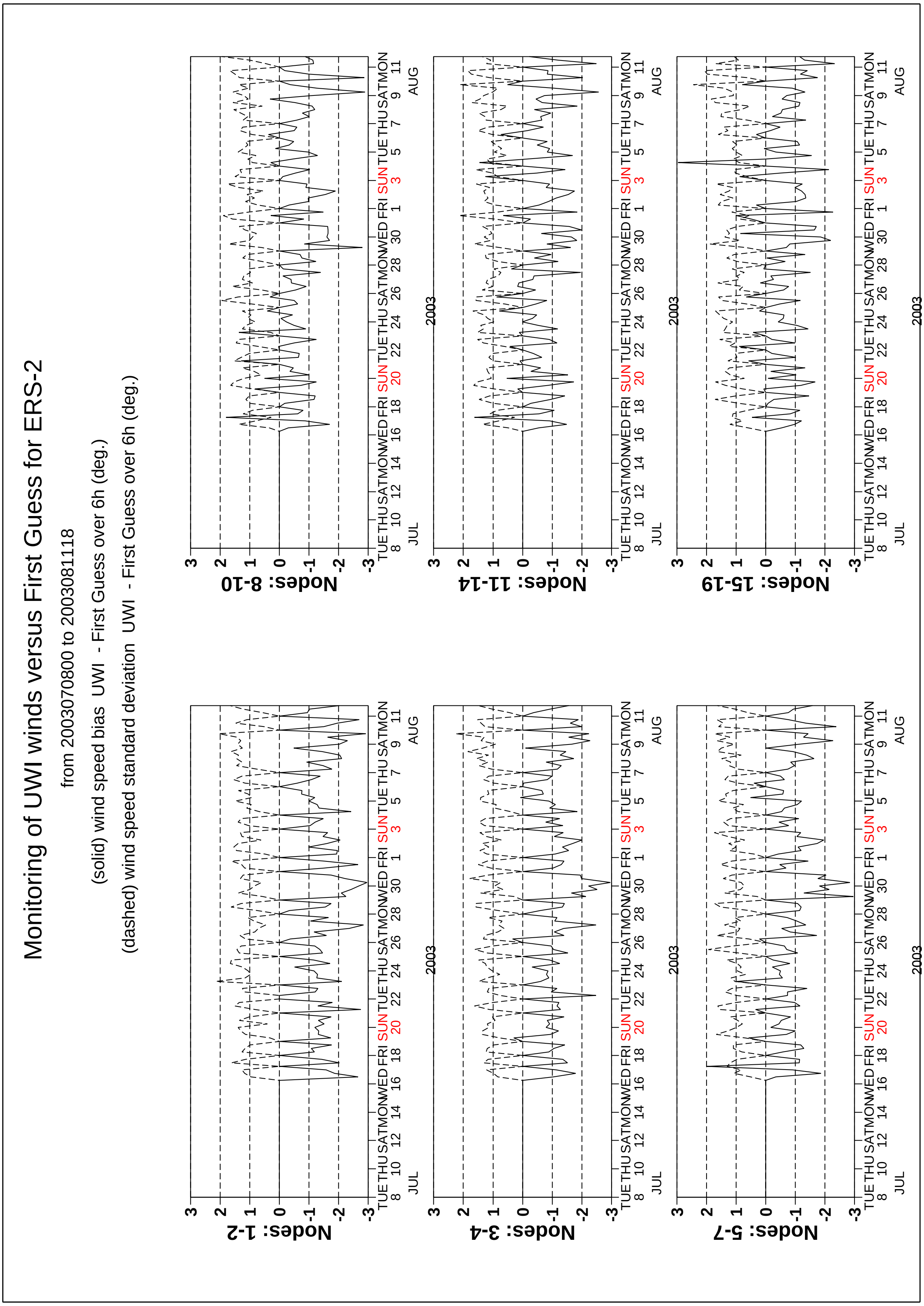
Monitoring of UWI winds versus First Guess for ERS-2
from 2003070800 to 2003081118
(solid) wind speed bias UWI - First Guess over 6h (deg.)
(dashed) wind speed standard deviation UWI - First Guess over 6h (deg.)
Nodes: 1-2
Nodes: 3-4
Nodes: 5-7
Nodes: 8-10
Nodes: 11-14
Nodes: 15-19
2003
JUL
AUG

Figure 4

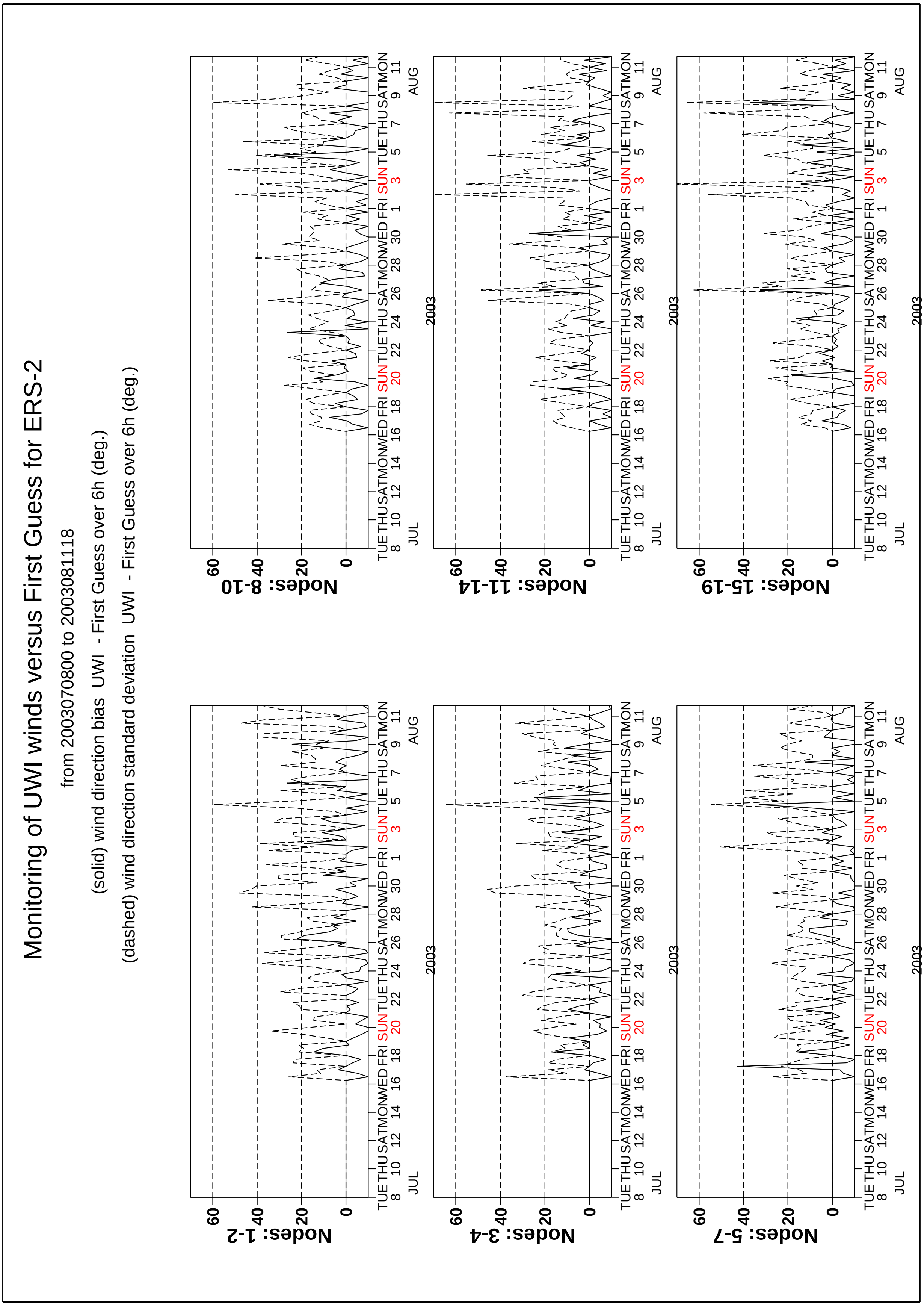
Monitoring of UWI winds versus First Guess for ERS-2
from 2003070800 to 2003081118
(solid) wind direction bias UWI - First Guess over 6h (deg.)
(dashed) wind direction standard deviation UWI - First Guess over 6h (deg.)
Nodes: 1-2
Nodes: 3-4
Nodes: 5-7
Nodes: 8-10
Nodes: 11-14
Nodes: 15-19
2003
JUL
AUG

Figure 5

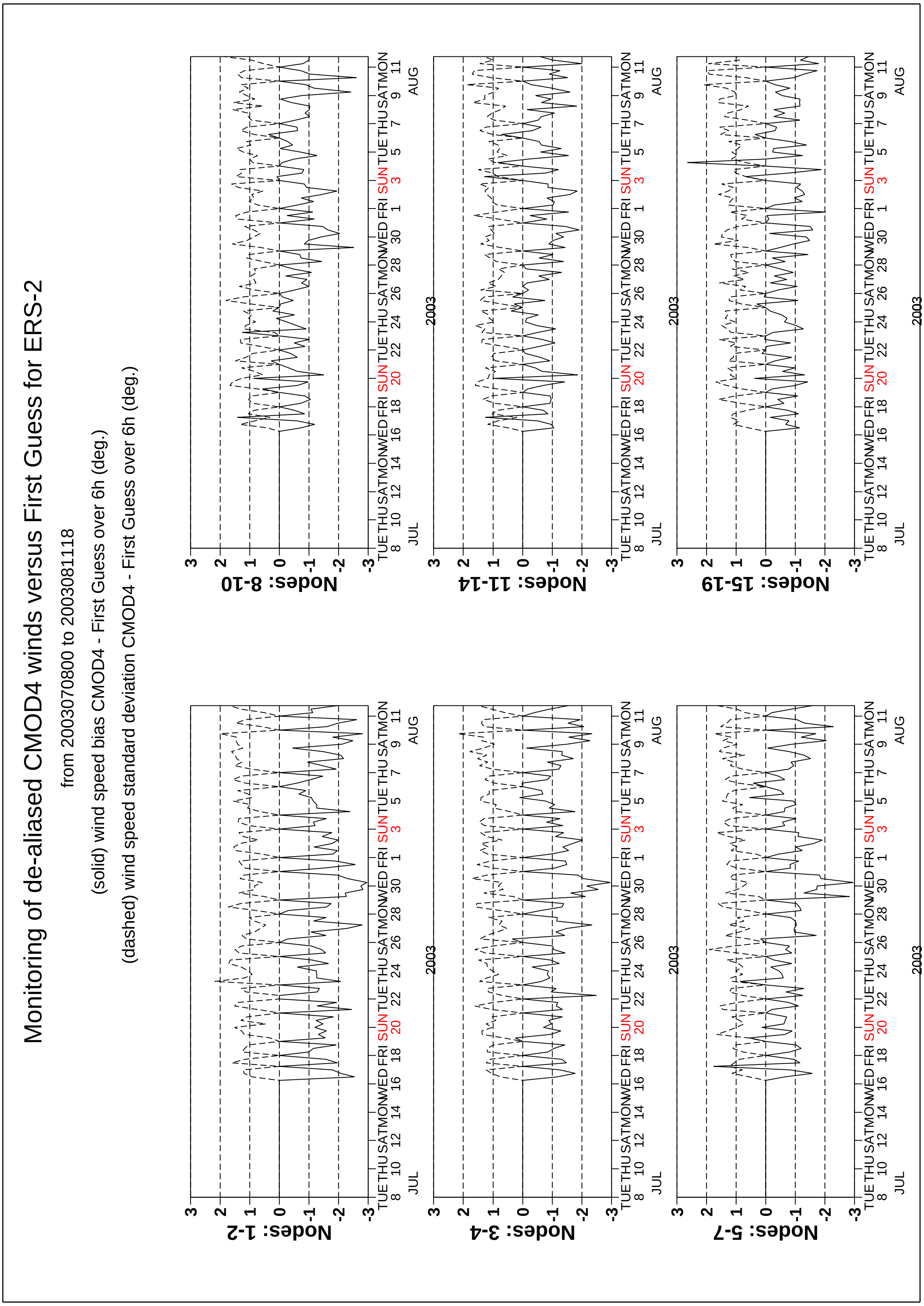
Monitoring of de-aliased CMOD4 winds versus First Guess for ERS-2
from 2003070800 to 2003081118
(solid) wind speed bias CMOD4 - First Guess over 6h (deg.)
(dashed) wind speed standard deviation CMOD4 - First Guess over 6h (deg.)
Nodes: 1-2
Nodes: 3-4
Nodes: 5-7
Nodes: 8-10
Nodes: 11-14
Nodes: 15-19
JUL
AUG
2003

Figure 6

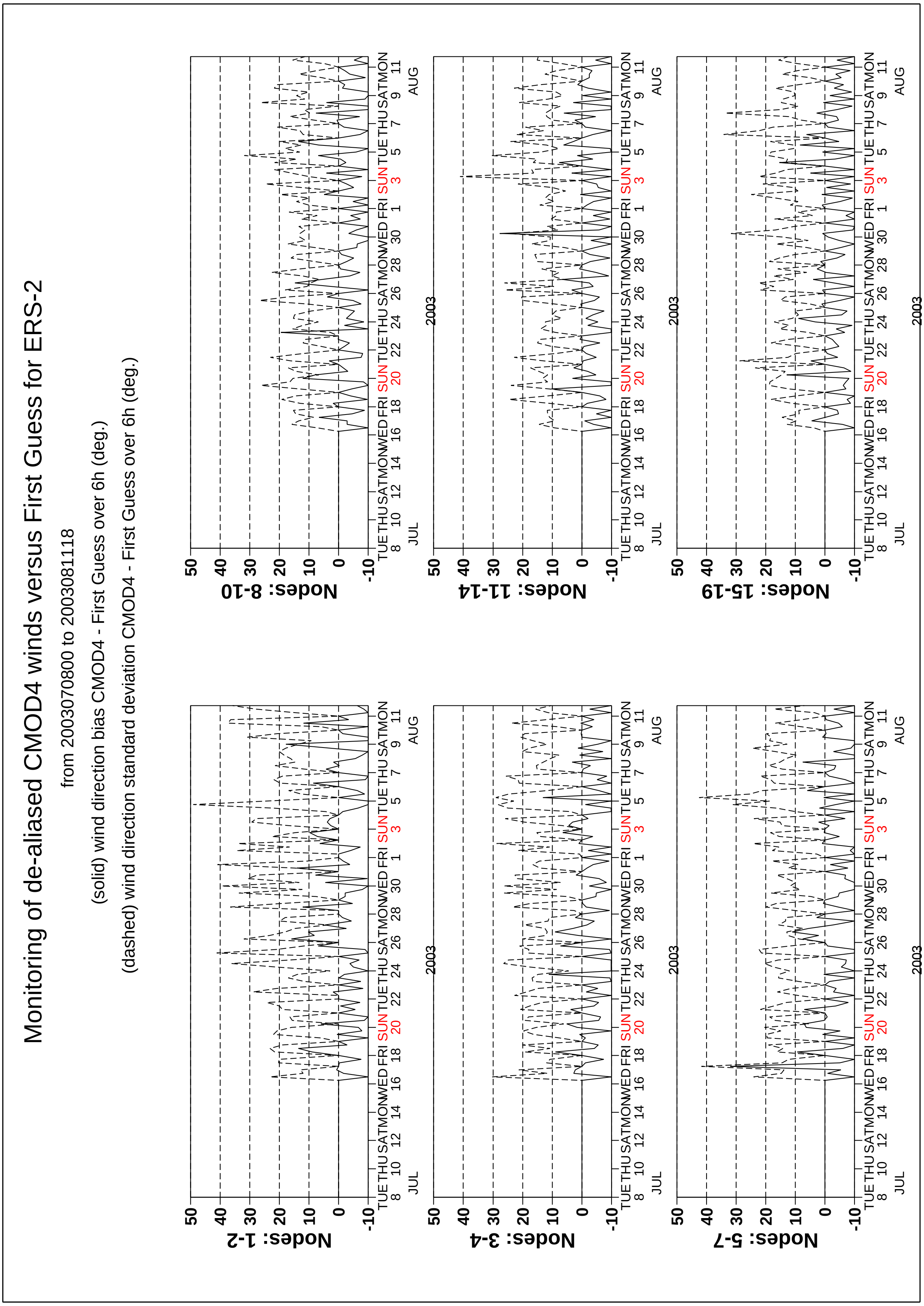
Monitoring of de-aliased CMOD4 winds versus First Guess for ERS-2
from 2003070800 to 2003081118
(solid) wind direction bias CMOD4 - First Guess over 6h (deg.)
(dashed) wind direction standard deviation CMOD4 - First Guess over 6h (deg.)
Nodes: 1-2
Nodes: 3-4
Nodes: 5-7
Nodes: 8-10
Nodes: 11-14
Nodes: 15-19
JUL
AUG
2003

Figure 7

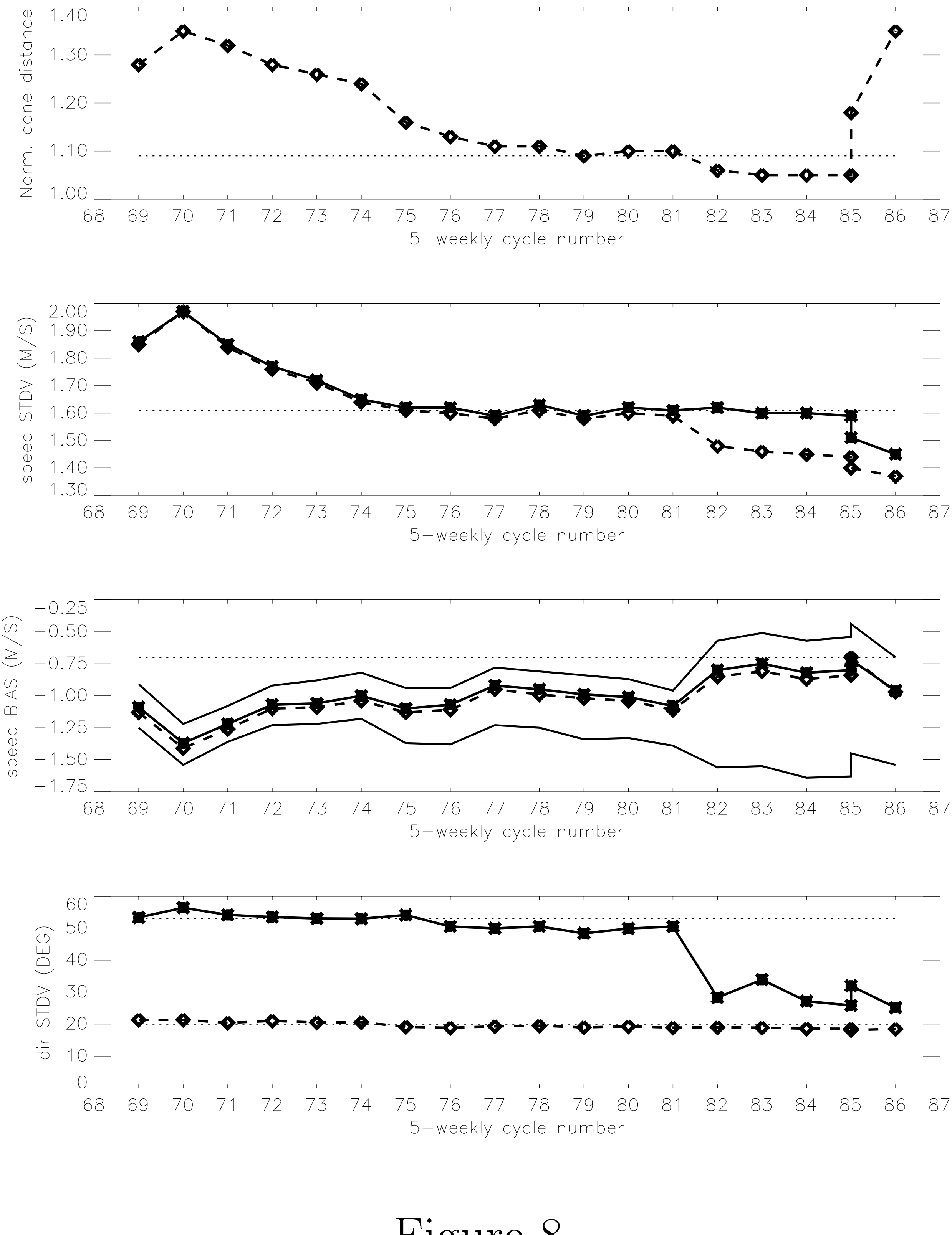
Norm. cone distance
5−weekly cycle number
speed STDV (M/S)
5−weekly cycle number
speed BIAS (M/S)
5−weekly cycle number
dir STDV (DEG)
5−weekly cycle number

Figure 8

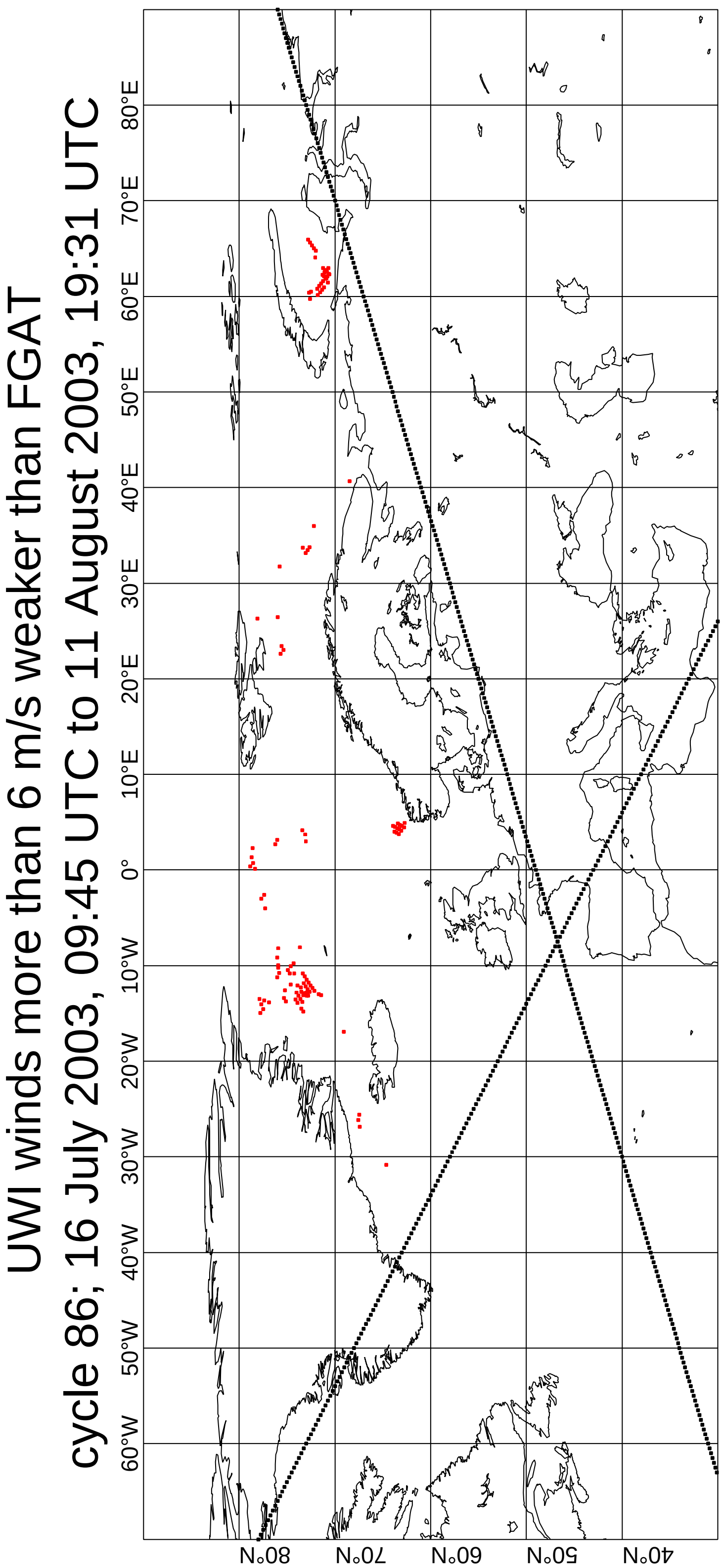
UWI winds more than 6 m/s weaker than FGAT
cycle 86; 16 July 2003, 09:45 UTC to 11 August 2003, 19:31 UTC
80°E
70°E
60°E
50°E
40°E
30°E
20°E
10°E
0°
10°W
20°W
30°W
40°W
50°W
60°W
80°N
70°N
60°N
50°N
40°N

Figure 9

UWI winds (red) versus FGAT winds (blue)
8 August 2003, 12:47 UTC

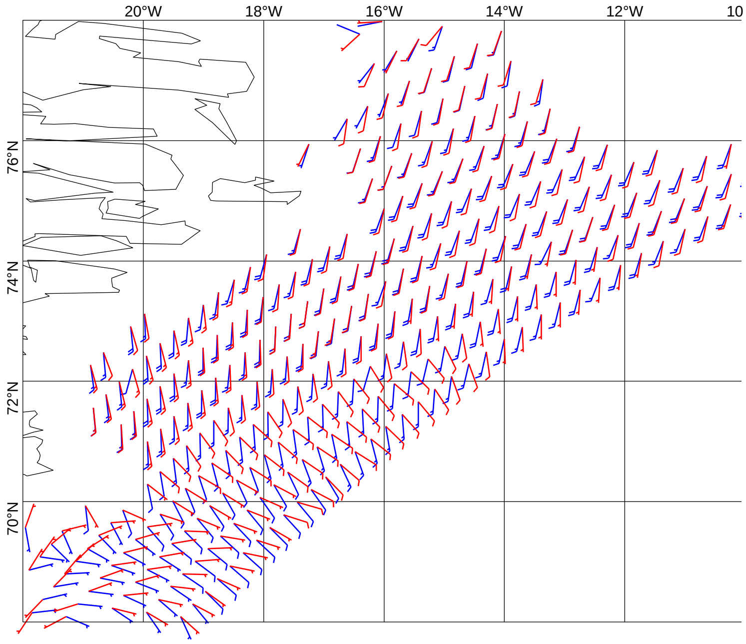

UWI winds (red) versus FGAT winds (blue)
30 July 2003, 10:51 UTC

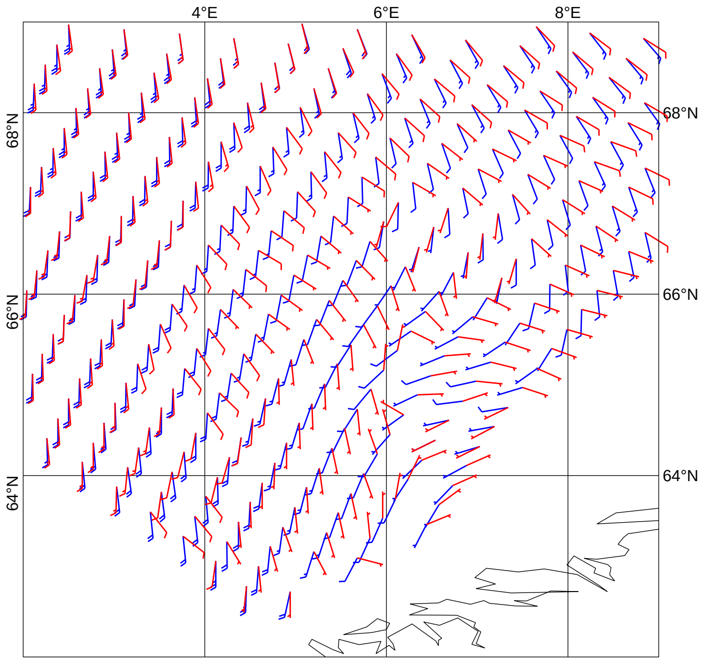

Figure 10

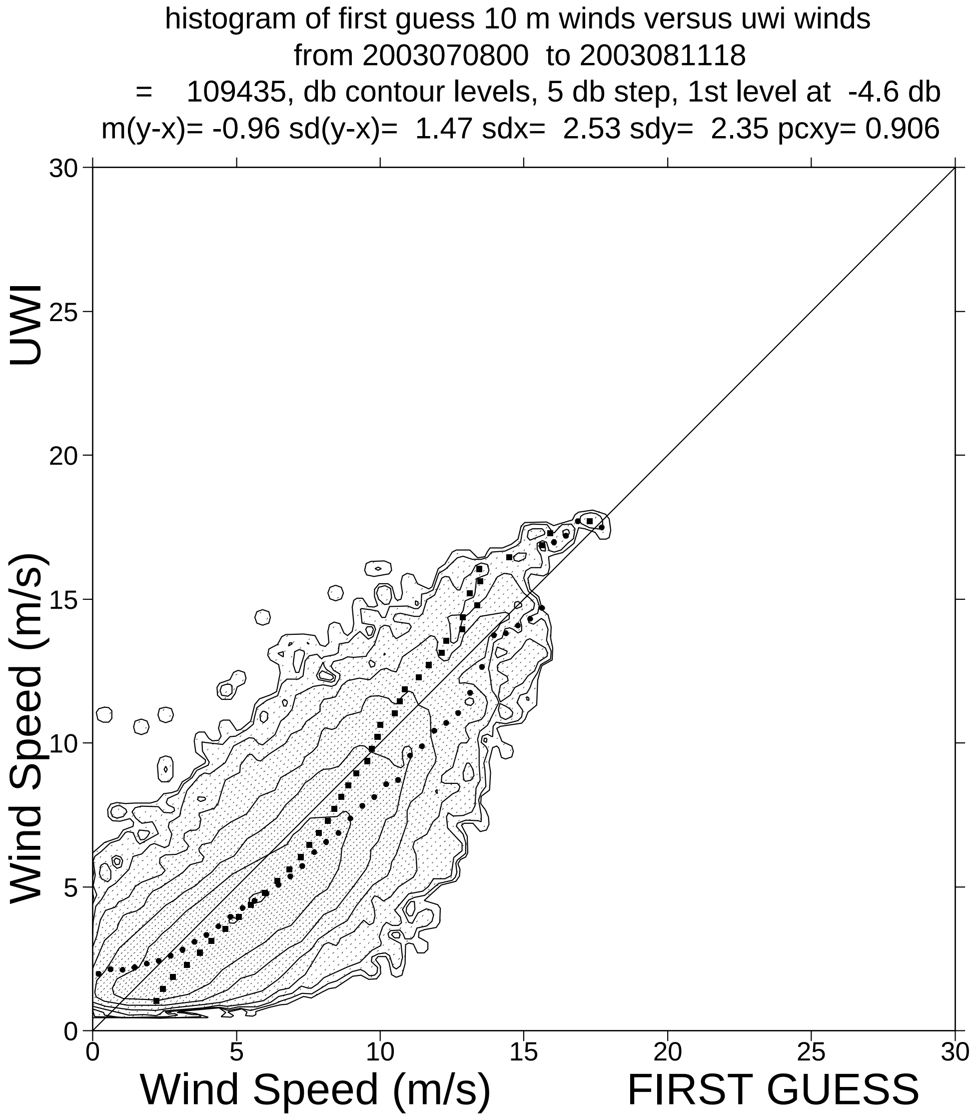
histogram of first guess 10 m winds versus uwi winds
from 2003070800 to 2003081118
= 109435, db contour levels, 5 db step, 1st level at -4.6 db
m(y-x)= -0.96 sd(y-x)= 1.47 sdx= 2.53 sdy= 2.35 pcxy= 0.906
UWI
Wind Speed (m/s)
Wind Speed (m/s)
FIRST GUESS
0
5
10
15
20
25
30

Figure 11

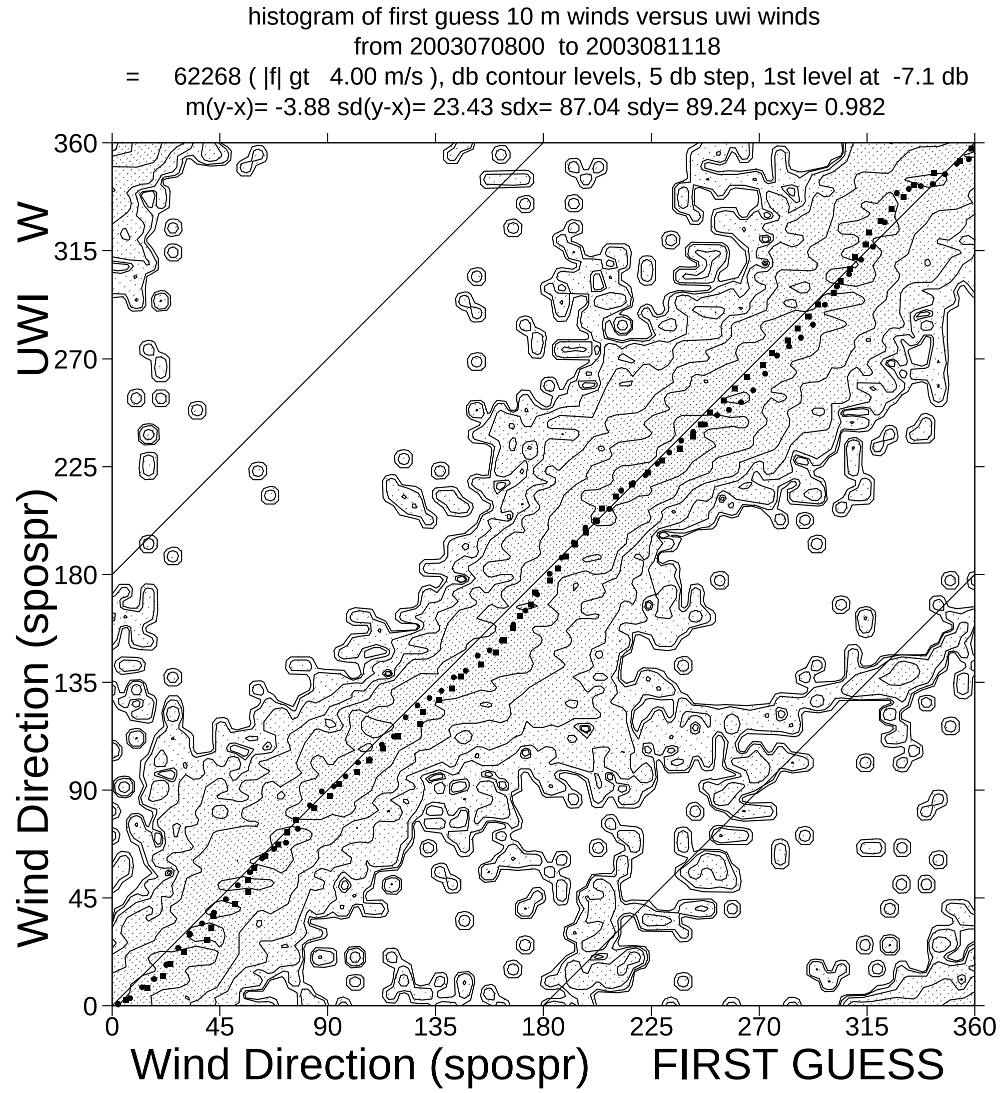
histogram of first guess 10 m winds versus uwi winds
from 2003070800 to 2003081118
= 62268 (|f| gt 4.00 m/s), db contour levels, 5 db step, 1st level at -7.1 db
m(y-x)= -3.88 sd(y-x)= 23.43 sdx= 87.04 sdy= 89.24 pcxy= 0.982
Wind Direction (spospr) UWI W
Wind Direction (spospr) FIRST GUESS
0
45
90
135
180
225
270
315
360

Figure 12

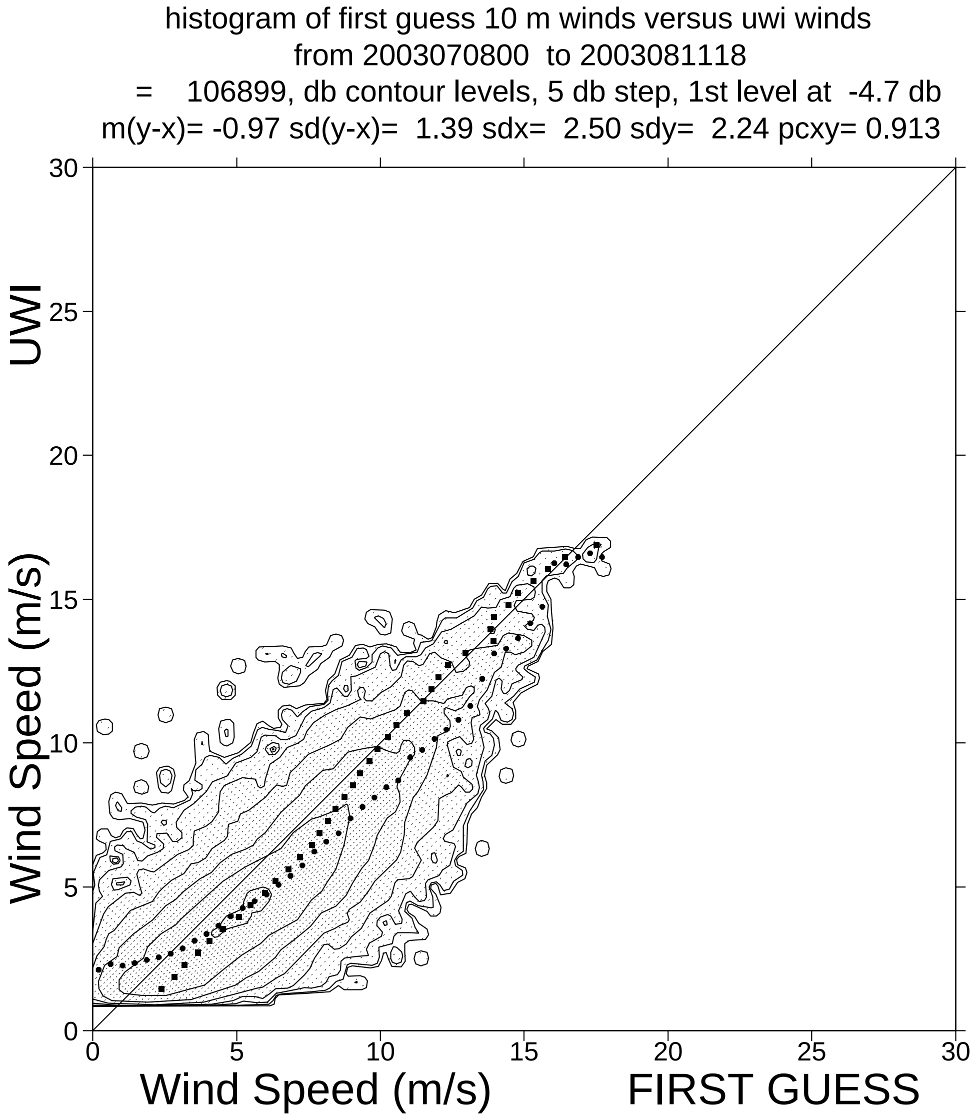
histogram of first guess 10 m winds versus uwi winds
from 2003070800 to 2003081118
= 106899, db contour levels, 5 db step, 1st level at -4.7 db
m(y-x)= -0.97 sd(y-x)= 1.39 sdx= 2.50 sdy= 2.24 pcxy= 0.913
UWI
Wind Speed (m/s)
Wind Speed (m/s)
FIRST GUESS
0
5
10
15
20
25
30

Figure 13

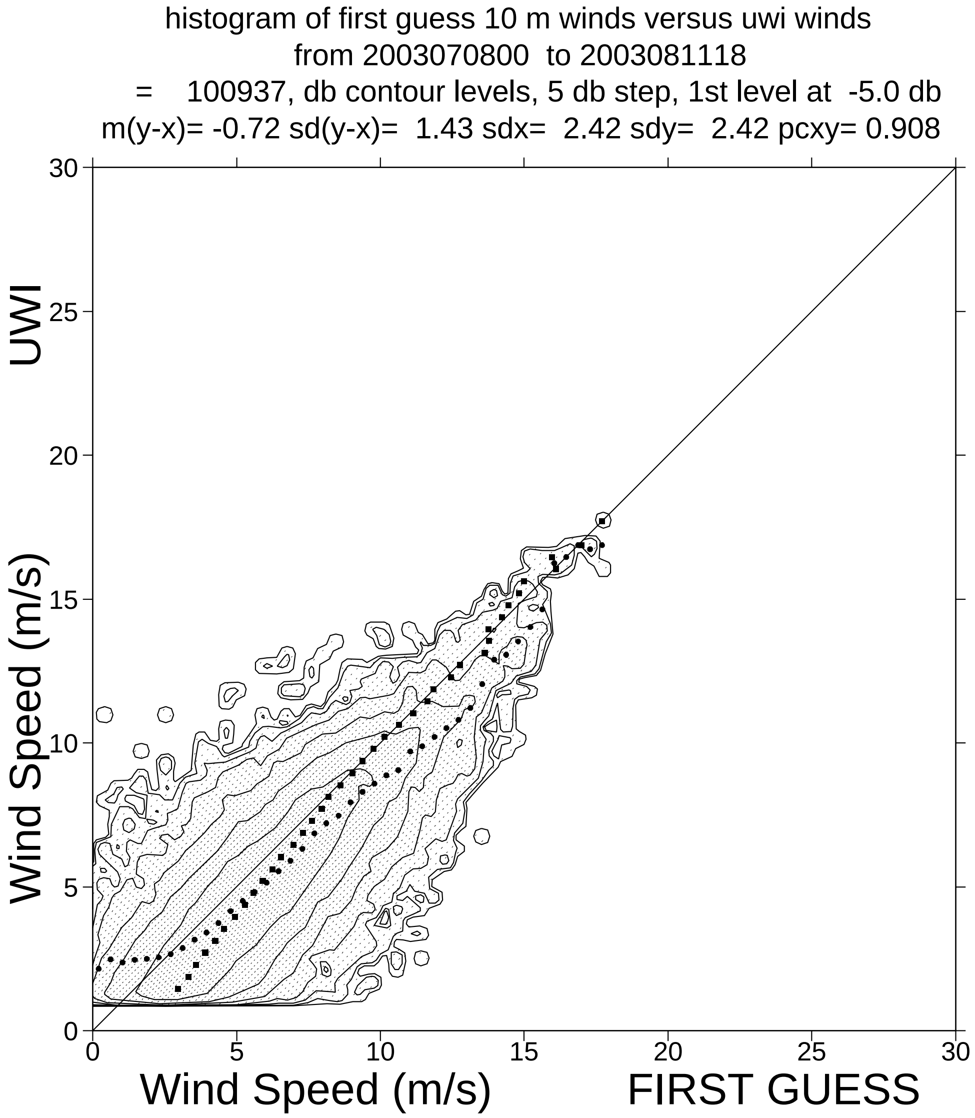
histogram of first guess 10 m winds versus uwi winds
from 2003070800 to 2003081118
= 100937, db contour levels, 5 db step, 1st level at -5.0 db
m(y-x)= -0.72 sd(y-x)= 1.43 sdx= 2.42 sdy= 2.42 pcxy= 0.908
UWI
Wind Speed (m/s)
Wind Speed (m/s)
FIRST GUESS
0
5
10
15
20
25
30

Figure 14